ELSEVIER

Coordination Chemistry Reviews
198 (2000) 3–20

COORDINATION CHEMISTRY REVIEWS

www.elsevier.com/locate/ccr

Active site models for galactose oxidase and related enzymes

Shinobu Itoh [1], Masayasu Taki, Shunichi Fukuzumi *

Department of Material and Life Science, Graduate School of Engineering, Osaka University, 2-1 Yamada-oka, Suita, Osaka 565-0871, Japan

Received 15 March 1999; accepted 21 July 1999

Contents

Abstract

Redox interaction between a transition-metal ion and a redox active amino acid side chain such as the phenol group of tyrosine in several enzymatic systems has been discovered to play a crucial role in biologically important processes. The tyrosyl radical, which directly coordinates to the copper ion center, has recently been found in the active sites of galactose oxidase (GAO) and glyoxal oxidase (GLO). In this article, model studies on the active site of the enzymes are reviewed by summarizing reported information about the physicochemical properties and the redox functions of the Cu(II) and Zn(II) complexes of the phenolate and phenoxyl radical forms of the cofactor models as well as the organic cofactor models themselves.

Keywords: Galactose oxidase; Glyoxal oxidase; Phenoxyl radical; Organic cofactor; Cu(II) complex; Alcohol oxidation

* Corresponding author. Tel.: +81-6-6879-7368; fax: +81-6-6879-7370.
E-mail address: fuzukumi@chem.eng.osaka-u.ac.jp (S. Fukuzumi)
[1] Also corresponding author.

0010-8545/00/$ - see front matter
PII: S0010-8545(99)00209-X

1. Introduction

The tyrosyl radical has now been well-recognized to play a crucial role in several enzymatic redox processes [1–3]. The R2 subunit of non-heme diiron enzyme ribonucleotide reductase from *E. coli* is one of the most well-characterized examples of such enzymes, where the tyrosyl radical, derived from Tyr 122 via the one-electron oxidation by the adjacent Fe(III)/Fe(IV)-oxo species (so-called intermediate X), initiates the nucleotide-reduction process [1,2]. Tyrosyl radicals are also involved as important intermediates in the redox processes of prostaglandin H synthase and photosystem II, in which ($porp^{+\bullet}$)Fe(IV)=O (porp = protoporphyrin IX) and a high valent manganese cluster are responsible for the tyrosyl radical formation, respectively [1,2]. The tyrosyl radical, which directly coordinates to the copper ion center, has recently been found in the active site of galactose oxidase (GAO, EC 1.1.3.9) that catalyzes the oxidation of D-galactose and primary alcohols to the corresponding aldehydes coupled to the reduction of O_2 to H_2O_2 (Eq. (1)) [4–15].

$$RCH_2OH + O_2 \rightarrow RCHO + H_2O_2 \quad (1)$$

The crystal structure of galactose oxidase at 1.7 Å resolution has clearly shown that the tyrosine residue (Tyr 272) is covalently bound to the sulfur atom of adjacent Cys 228 at the α-position of the phenol ring as illustrated in Scheme 1 [6,7]. This built-in organic cofactor serves as a one-electron redox center by shuttling between the phenol and phenoxyl radical forms during the course of the redox cycle; the alcohol-oxidation and the O_2-reduction [8–12]. Thus, the active species (fully oxidized state) of the enzyme is the Cu(II)–phenoxyl radical of Tyr 272 that can oxidize alcohols to the corresponding aldehydes by the following mechanism: (i) deprotonation from the –OH group of the bound substrates by the phenolate group of Tyr 495, (ii) inner-sphere electron transfer from the deprotonated substrate to Cu(II), and (iii) α-hydrogen atom abstraction of the resulting ketyl radical by the phenoxyl radical of Tyr 272 species (the ordering of electron transfer and hydrogen atom abstraction steps could be reversed) [11–15]. It is further proposed that the fully oxidized state is reproduced from the fully reduced state [Cu(I)–phenol] by the reaction with molecular oxygen that is transformed into hydrogen peroxide as shown in Eq. (1). The interconversion between Cu(I) and Cu(II) states has also been demonstrated by X-ray absorption spectroscopy [16,17].

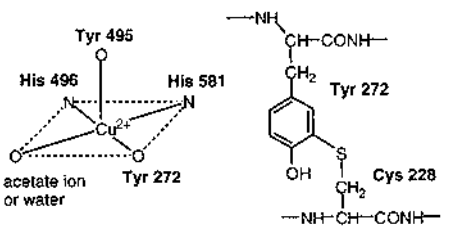

Scheme 1.

Such a phenoxyl radical–copper catalytic motif has also been found in glyoxal oxidase (GLO) from *Phanerochaete chrysosporium* and in the prokaryotic FbfB protein [18–20].

The development of synthetic analogues of metalloenzyme active sites has provided valuable insight into structures, physicochemical properties, and functions of active intermediates in enzymatic reactions, which are often obscured by the huge peptide backbones of the native enzymes. Model studies on GAO and the related enzymes have also given valuable information about (i) the electronic effects of the thioether group of the cofactor, (ii) physicochemical properties of phenoxyl radical species of the cofactor both in the metal-free form and in the metal complexes, and (iii) the catalytic alcohol oxidation by Cu(II)–phenoxyl radical complexes. The purpose of this review article is to summarize such studies. Copper complexes of simple phenol derivatives containing a metal binding site are not included in this article.

2. Organic cofactor models (apo-enzyme model)

2.1. Neutral and anionic (phenolate) forms

One of the most interesting features of the enzyme is the existence of the thioether linkage between Tyr 272 and Cys 228 (Scheme 1). Then a question arises why galactose oxidase and the related enzymes employ such a modified amino acid residue instead of a simple tyrosine. The redox potential of galactose oxidase is estimated to be 400–500 mV vs. NHE [10], that is significantly lower than that of free tyrosine in solution (930 mV) or tyrosine in enzymatic systems (760–1000 mV) [21,22]. Such a negative shift of the redox potential has been attributed in part to the electron-donating nature of the thioether group of the cofactor [23]. On the other hand, Babcock, Whittaker, and co-workers reported that about 25% of the spin density delocalizes into the sulfur atom of Cys 228 in the radical state of the apo-enzyme, thus demonstrating the electron-sharing conjugative effect of the thioether group of the cofactor [24,25]. In order to obtain further insight into the electronic effects of the thioether group of the cofactor, physicochemical properties of simple cofactor models (**1H** and **2H**) have been examined (vide infra) [24,26–28].

Selected analytical data of cofactor models **1H** and **2H** are summarized in Table 1 together with those of *p*-cresol (**3H**) for comparison [28]. The up-field shifts of the aromatic protons of **1H** and **2H** (except H-3 of **1H**) as compared to those of **3H** indicate that the methylthio substituent has a somewhat *electron-donating nature* in both the neutral and anionic forms.

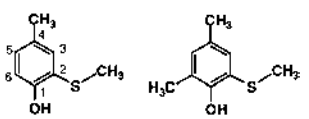

1H **2H**

Table 1
Selected analytical data of **1H**, **2H** and *p*-cresol (**3H**) and their anionic forms [28]

Compound	^{1}H-NMR/δ[a]			UV–vis λ_{max} /nm[b]		pK_a[c]	E°_{ox} vs. SCE /mV[d]
	H-3	H-5	OH				
1H	7.12	6.91	6.87	250	295	9.6	+1106
2H	7.07	6.89	6.62	252	292	9.9	+955
3H	7.00	7.00	6.66	223	280	10.4	+1474
$\mathbf{1}^-$	6.65	6.57	–	268[e]	338	–	−246
$\mathbf{2}^-$	6.53	6.52	–	270[e]	334	–	−326
$\mathbf{3}^-$	6.72	6.72	–	251	321	–	−146

[a] 50 mM in CD_3CN; the phenolate form was generated in the NMR tube by adding 4 equiv. of NMe_4OH.
[b] In CH_3CN; the phenolate form was generated in the UV cell by adding 10-fold excess of NMe_4OH.
[c] Determined by ordinary spectrophotometric titration in a 0.1 M aqueous buffer solution containing 1% CH_3OH.
[d] One-electron oxidation potential determined by SHACV method in CH_3CN containing 0.1 M NBu_4ClO_4; the anionic form was generated in the cell by adding a slight excess of NMe_4OH.
[e] Shoulder.

Since the phenol derivatives gave irreversible cyclic voltammograms due to the instability of the corresponding phenoxyl radicals in solution, the one-electron redox potentials have been determined by the SHACV (second-harmonic ac voltammetry) method [28]. The E°_{ox} values thus determined are listed in Table 1. Introduction of methylthio group into the ortho position of the phenol ring causes a negative shift of E°_{ox} by hundreds mV, also suggesting the electron-donating nature of the substituent.

The pK_a values of the phenolic protons seems somehow abnormal, since the methylthio substitution causes an increase in the acidity of the phenol proton by about one pH unit (**1H**, 9.6; **3H**, 10.4) despite the electron-donating nature of the substituent. A decrease in the pK_a value of *p*-alkylthio substituted phenols as compared to that of phenol itself was also reported [29]. This phenomenon has been explained by taking account of the fact that the sulfide group can stabilize negative charge when connected with a conjugated system, so-called 2pπ–3dπ conjugation [23]. The PM3 calculations supported such possibility; net atomic charges of the sulfur atoms in **1H** and $\mathbf{1}^-$ are +0.064 and −0.04, respectively [27,28].

2.2. Metal-free phenoxyl radicals

Absorption spectra of the radical species of compound **1H** and *p*-cresol (**3H**) can be obtained by pulse radiolysis in an alkaline aqueous solution (Fig. 1) [27,28]. *p*-Cresol shows a characteristic absorption band at around 400 nm due to the phenoxyl radical [30]. In contrast to the case of *p*-cresol, a model compound $\mathbf{1}^\bullet$ gives a very broad absorption band from 600 to 900 nm together with strong bands at around 350 and 400 nm (Fig. 1). The absorption spectrum of $\mathbf{1}^\bullet$ in solution is

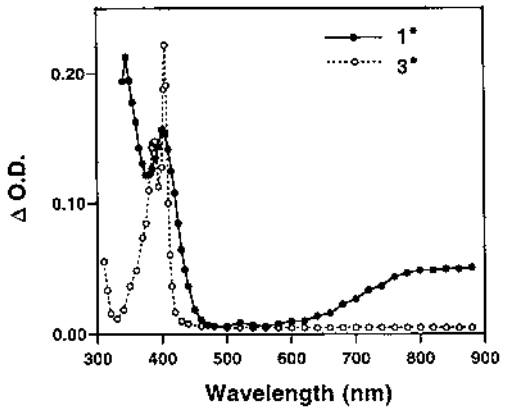

Fig. 1. Transient absorption spectra obtained by the pulse radiolysis of **1H** and **3H** in an N_2O-saturated aqueous solution (pH 11) containing NaN_3 (0.1 M) [28].

very close to that of the oxidized apo-galactose oxidase [10], indicating that **1H** is a good model of the active site cofactor of apo-galactose oxidase [27,28]. Whittaker and co-workers obtained essentially the same spectrum of **1•** by UV-irradiation in propionitrile–butyronitrile matrix at 77 K [26].

Well-resolved solution ESR spectra of **1•** and **2•** were obtained under photolysis in the ESR cavity of a solution of **1H** or **2H** containing dicumyl peroxide [28]. In Fig. 2 are shown the solution ESR spectra of **1•** and **2•**. The *g* values of **1•** and **2•** (2.0060 and 2.0052, respectively) are very close to that of the cofactor radical (2.0055) in the apo-enzyme [19]. Hyperfine coupling constants (hfc) determined by

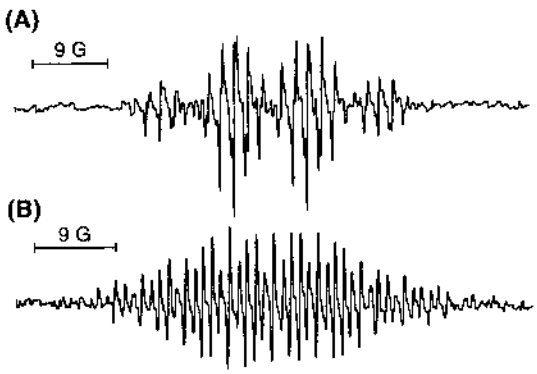

Fig. 2. (A) A solution ESR spectrum of **1•** obtained under photolysis in the ESR cavity of a toluene solution of **1H** (2.0 M) containing 1.0 M dicumyl peroxide at −30°C; microwave frequency 9.09 GHz; modulation frequency 100 kHz; modulation amplitude 0.5 G; microwave power 8 mW, and (B) a solution ESR spectrum of **2•** obtained under photolysis in the ESR cavity of a benezene solution of **2H** (2.0 M) containing 1.0 M dicumyl peroxide at 25°C; microwave frequency 9.45 GHz; modulation frequency 100 kHz; modulation amplitude 0.5 G; microwave power 8 mW [28].

Table 2
Isotopic g values and proton hyperfine coupling constants (G) for the phenoxyl radicals [28]

Radical	g	A_2	$A_{3\text{-H}}$	$A_{4\text{-Me}}$	$A_{5\text{-H}}$	A_6
1•[a]	2.0060	1.7[e]	0.3	8.6	0.5	3.1[g]
2•[b]	2.0052	2.8[e]	0.7	9.6	0.9	3.9[h]
3•[c]	–[d]	6.1[f]	1.4	12.3	1.4	6.1[g]

[a] At −30°C in toluene.
[b] At 25°C in benzene.
[c] Taken from: W.T. Dixon, R.O.C. Norman, J. Chem. Soc. (1964) 4857.
[d] Not reported.
[e] For 2-SCH_3.
[f] For 2-H.
[g] For 6-H.
[h] For 6-CH_3.

the computer simulation for **1**• and **2**• are listed in Table 2 together with those of phenoxyl radical of *p*-cresol (**3**•). The isotropic hfc values for **1**• in solution agree with those estimated from the reported anisotropic hfc values obtained from the powder ESR spectrum [24]. It is obvious that the total spin density at the 3-, 4-, 5-, and 6-positions in **1**• and **2**• decreases significantly as compared to that of **3**•. These results indicate that a relatively large amount of the spin density delocalizes into the sulfur atom of the methylthio group [28].

Semiempirical molecular orbital calculations (PM3) on compound **1H** and its anionic (**1**$^-$) and radical (**1**•) forms have revealed the electronic effect more clearly [27,28]. Fig. 3(A) shows the bond orders in the optimized structures of **1H**, **1**$^-$, and **1**•. The bond orders of C(1)–O(8), C(5)–C(6), and C(2)–S(9) increase in going from **1H** to **1**•, while those of C(1)–C(2), C(4)–C(5), and C(1)–C(6) decrease. These results indicate that the *o*-quinonoid canonical form (Scheme 2) partially contributes to the stabilization of the radical species, though the bond-order changes of C(2)–C(3) and C(3)–C(4) are very small. The calculated spin density of **1**• is compared with that of the phenoxyl radical of *p*-cresol (**3**•) in Fig. 3(B) [27,28]. The spin densities at C(4), C(6), and O(8) are diminished by introduction of a methylthio substituent into the 2-position of *p*-cresol, while the unpaired electron is distributed among C(2) and S(9) to a considerable extent. These results are consistent with the well documented *electron-sharing conjugative effect* of sulfide groups (Scheme 2) [23].

The PM3 calculations indicate that in the optimized molecular geometry of **1**•, the methylthio group stays in the same plane of the aromatic ring, while the methyl group moves away from the plane in **1H** and **1**$^-$ [27,28]. The dihedral angles defined by C(1)–C(2)–S(9)–C(10) in **1H** and **1**$^-$ are 70 and 60°, respectively [27,28]. The difference in the optimized structure between **1**• and **1H** or **1**$^-$ suggests an increasing sp^2-character of the sulfur atom in the radical state, and thus, the contribution of the *o*-quinonoid canonical form as illustrated in Scheme 2. The partial double bond character of the thioether linkage in the native cofactor was

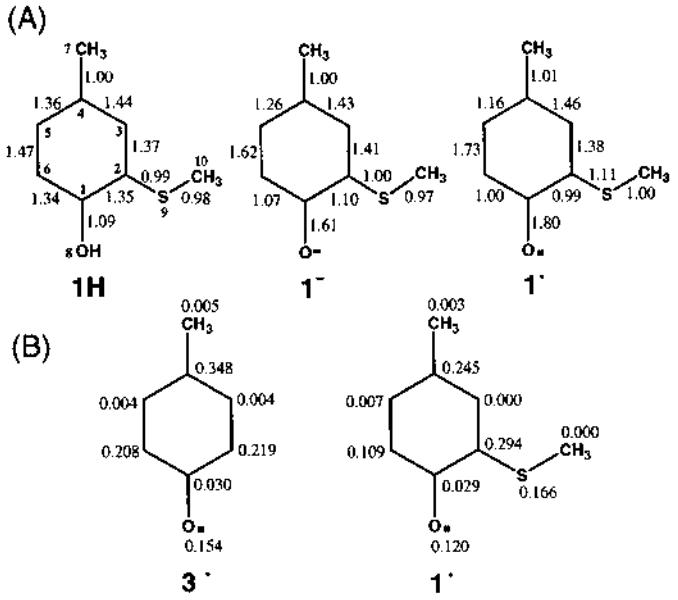

Fig. 3. (A) Bond orders of **1H**, $\mathbf{1}^-$, and $\mathbf{1}^\bullet$ calculated by the PM3 method [27,28]. (B) Spin densities of $\mathbf{3}^\bullet$ and $\mathbf{1}^\bullet$ calculated by the PM3 method [27,28].

also suggested by its similar molecular geometry in the enzyme active site [6]. The relatively large negative shift of the E°_{ox} values of the model compounds having methylthio group as compared to the corresponding phenol derivatives without the substituent (Table 1) can also be attributed to both the electron-donating nature and the radical stabilizing effect by electron spin delocalization into the methylthio group, that is called electron-sharing conjugative effect. The SOMO and LUMO of $\mathbf{1}^\bullet$ were also calculated by the PM3 method [28]. The SOMO orbital is located mainly on the benzene ring [C(2), C(4), and C(6)], while the LUMO orbital remains around the methylthio group. Thus, the very broad absorbance of $\mathbf{1}^\bullet$ in Fig. 1 could be attributed to an intramolecular charge-transfer from the benzene ring to the methylthio group.

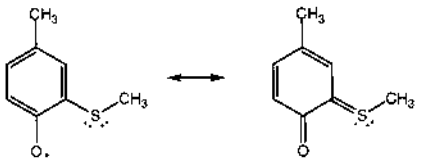

Scheme 2.

3. Copper(II)–phenolate complexes (resting state model)

The first copper(II) complex of the cofactor model was reported by Whittaker and co-workers in 1993 [26,31]. It is a ternary complex consisting of a copper(II) ion, $\mathbf{1}^-$ as the cofactor model, and *N*,*N*,*N*′,*N*′,*N*″-pentamethyldiethylenetriamine (PMDT) as a supporting ligand, $[Cu^{II}(PMDT)(\mathbf{1}^-)](ClO_4^-)\cdot CH_3OH$ [26]. The copper complex has a square pyramidal structure in which basal plane is occupied by three nitrogen atoms of PMDT and the phenolate oxygen of $\mathbf{1}^-$ [26]. The sulfur atom of the methylthio group of $\mathbf{1}^-$, however, coordinates to the copper ion from the axial position, making the coordination geometry somewhat different from that of the native enzyme; in the enzymatic system, there is no coordinative interaction between the sulfur atom and Cu(II) [6]. This complex has a relatively weak phenolate to Cu(II) LMCT band at 525 nm ($\varepsilon = 535\ M^{-1}\ cm^{-1}$) together with a d–d band of Cu(II) at 734 nm ($\varepsilon = 535\ M^{-1}\ cm^{-1}$) [26]. Treatment of this complex in boiling CH_3CN gave an *ortho–ortho* coupled dimer of **1H** ($\mathbf{1_2H_2}$), indicating an inner-sphere electron transfer from $\mathbf{1}^-$ to Cu(II) to generate $\mathbf{1}^\bullet$ and Cu(I) (Scheme 3) [26]. Instability of the radical intermediate has, however, precluded the detailed studies on the redox reaction of the model complex.

Whittaker and co-workers have extended their model studies of GAO by developing a new ligand $\mathbf{4H_2}$, in which the cofactor moiety is incorporated into the metal binding site consisting of a tertiary amine nitrogen, 2-pyridyl group, and another phenol group as shown below [32]. This ligand has been designed to mimic the N_2O_2 donor set of the native enzyme [6]. A copper(II) complex of this ligand was obtained in a dimeric form, $[Cu_2^{II}(\mathbf{4}^{2-})_2]$ containing a $Cu_2^{II}O_2$ core as the linker group. The dimeric complex could be converted into the monomer, $[Cu^{II}(\mathbf{4}^{2-})(Py)]$, by adding an external ligand such as pyridine (Py) [32]. The generated monomer complex exhibited a LMCT band at 475 nm ($\varepsilon = 1430\ M^{-1}\ cm^{-1}$) due to the equatorial phenolate coordination and showed a ESR spectrum typical for a distorted square pyramidal structure [32]. The monomer complex shows irreversible anodic peaks at $+116$ and $+463$ mV vs. $Ag/AgNO_3$ ($+753$ mV vs. SCE) in CH_3CN due to the one-electron oxidation of the phenolate groups [32]. Irreversibility of the electrochemical oxidation indicates that the phenoxyl radical of the cofactor moiety is not so stable at ambient temperature.

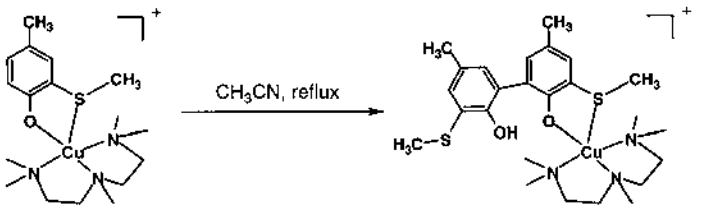

$[Cu^{II}(PMDT)(1^-)]^+$

Scheme 3.

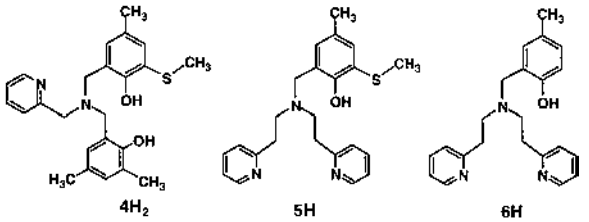

We have observed similar chemistry using ligand **5H** [28]. The copper(II) complex of **5H** was obtained as a dimeric form, $[Cu^{II}_2(\mathbf{5}^-)_2](PF^-_6)_2$ (Fig. 4), that was converted into the monomer, $[Cu^{II}(\mathbf{5}^-)(Py)]^+$, by the addition of an external ligand such as pyridine (Py) [28]. The monomer complex showed a phenolate to Cu(II) LMCT absorption at 540 nm ($\varepsilon = 1320\ M^{-1}\ cm^{-1}$) and exhibited an ESR spectrum that is typical for a square pyramidal geometry of Cu(II) [28].

The fast-scan cyclic voltammetry of $[Cu^{II}(\mathbf{5}^-)(Py)]^+$ gave a reversible wave at $+370$ mV vs. $Ag/AgNO_3$ ($+660$ mV vs. SCE) at a scan rate of 100 V s^{-1} [28]. However, no reversible wave for complex $[Cu^{II}(\mathbf{6}^-)(Py)]^+$, in which ligand **6H** has no methylthio group, has been observed even at a faster scan rate (300 V s^{-1}) [28]. This result clearly indicates that the stability of the radical species of $[Cu^{II}(\mathbf{5}^-)$-

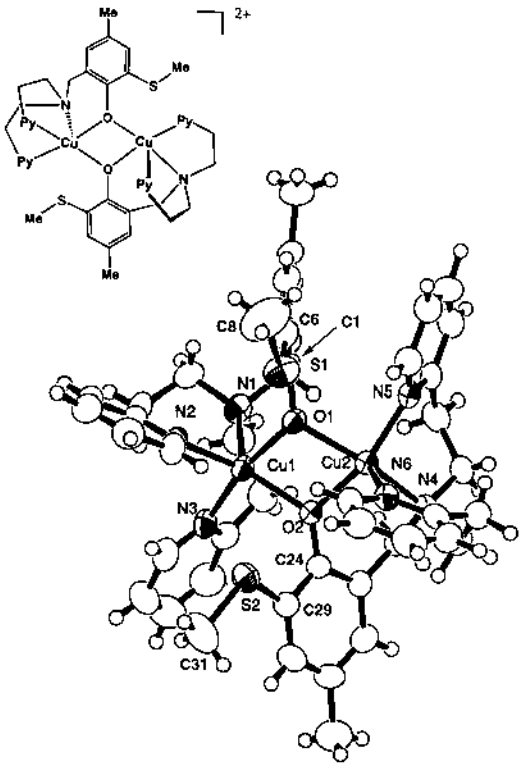

Fig. 4. ORTEP drawing of $[Cu^{II}_2(\mathbf{5}^-)_2](PF_6)_2$. The counter anions are omitted for simplicity [28].

$(Py)]^+$ is higher than that of $[Cu^{II}(\mathbf{6}^-)(Py)]^+$ due to the radical stabilizing effect of the methylthio group as mentioned above. Furthermore, the oxidation peak potential of $[Cu^{II}(\mathbf{5}^-)(Py)]^+$ is about 200 mV lower than that of $[Cu^{II}(\mathbf{6}^-)(Py)]^+$ (623 mV vs. $Ag/AgNO_3$) [28]. This result can also be explained by taking account of both the electron-donation effect and electron-sharing conjugation (radical stabilization) effect by the methylthio group as mentioned above. Delocalization of the negative charge of the phenolate moiety into the methylthio substituent also resulted in a positive shift of the redox potential at the copper site (-622 and -591 mV $Ag/AgNO_3$ for $[Cu^{II}(\mathbf{6}^-)(Py)]^+$ and $[Cu^{II}(\mathbf{5}^-)(Py)]^+$, respectively) [28].

1,4,7-Triazacyclononane (TACN) and its derivatives have been widely used as the ligands in coordination chemistry. Although several kinds of transition-metal complexes supported by the TACN ligands involving one, two or three phenol groups have been reported by Wieghardt and co-workers [33], we herein focused on the Cu(II) and Zn(II) complexes of the TACN derivatives as the model for GAO [34–36].

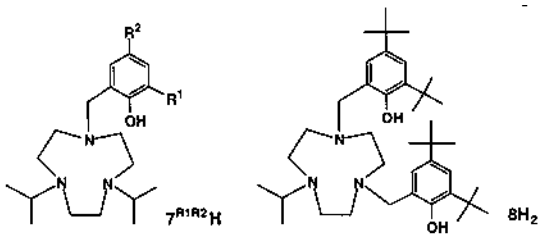

All the ligands ($R^1 = Me$ or ^{t}Bu and $R^2 = Me$, ^{t}Bu, OMe, or SMe) afforded monomeric penta-coordinated Cu(II) complexes with a square pyramidal structure, in which the phenolate group occupies the equatorial position [34,35]. The copper(II) complexes exhibit the ligand to metal charge transfer (LMCT) transition at 450–530 nm ($\varepsilon = 1000$–2000 M^{-1} cm^{-1}) and the ESR spectra (frozen solution at 77 K) are consistent with a $d_{x^2-y^2}$ ground state ($g_{\|} > g_{\perp} > 2.0$, $A_{\|} = 150$–170 G) with a minor rhombic perturbation [35]. As expected from the results of $[Cu^{II}(\mathbf{4}^{2-})$-$(Py)]$ [32], the Cu(II) and Zn(II) complexes of the ligands containing *p*-methyl substituent ($R^2 = Me$) exhibit an irreversible oxidation process in the ordinary cyclic voltammetric measurement [35]. However, the Cu(II) and Zn(II) complexes

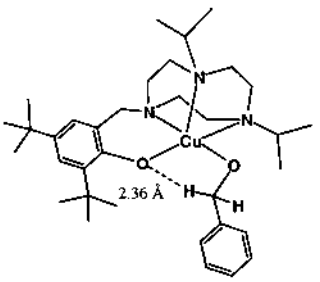

Scheme 4.

of the *p-tert*-butyl substituted ligands, $\mathbf{7}^{R\,{}^{t}Bu}\mathbf{H}$ and $\mathbf{8H}_2$ show a reversible redox process at around 500 mV vs. SCE [35].

An alcohol adduct of the Cu(II) complex of $\mathbf{7}^{{}^{t}Bu^{2}}\mathbf{H}$ was successfully isolated and its structure has been determined by X-ray crystallographic analysis [34]. As illustrated in Scheme 4, the ternary complex has a square pyramidal structure, in which the basal plane is occupied by two nitrogen atoms of the ligand, the phenolate oxygen of the cofactor moiety, and the oxygen atom of the alkoxide, while the third nitrogen atom of the ligand coordinates to Cu(II) from the axial direction [34]. Bulk electrolysis of the benzyl alcohol adduct (+ 370 mV vs. SCE in CH_3CN) produced benzaldehyde in 46% yield [34]. Although the mechanistic details are not clear at present, it is interesting to note that there is a hydrogen bonding interaction between one of the benzylic proton of the bound substrate and the phenolate oxygen of the cofactor, which may play an important role in the alcohol oxidation by phenoxyl radical species.

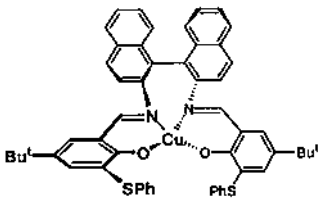

$[Cu^{II}(9^{2-})]$

Scheme 5.

A series of Cu(II) complexes with *N*-alkylsalicylaldimine derivatives have also been reported as the model for GAO [37–39]. The Cu(II) diphenolate complex has a significantly distorted square planar coordination geometry with a N_2O_2 donor set [37–39]. The ESR spectra of the Cu(II) complexes are similar to that of GAO, whereas the electronic spectra and the electrochemical properties differ significantly [37] (Scheme 5).

Cu(II) complexes having an axially coordinated phenolate group (Scheme 6, left, $X = SCN^-$, AcO^-) have been reported as models for axially coordinated Tyr 495 in the active site of GAO (see Scheme 1) [40,41]. The unusual occupation of the

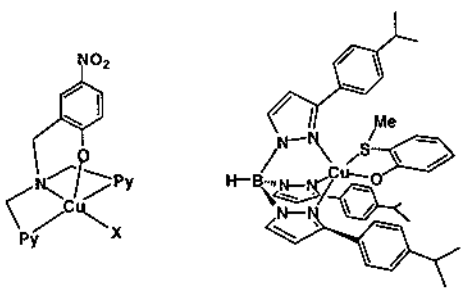

Scheme 6.

phenolate group in the axial site has been attributed to the steric constraint at copper imposed by the 5,5,6-chelate ring sequence [40,41]. The π–π interaction between the organic cofactor (Tyr 272) and the indole ring of Trp 290 (see Refs. [6,7]) has also been examined using Cu(II) complexes of tris(3-arylpyrazolyl)hydroborate ligands as shown in Scheme 6 (right) [42,43]. Comparison of the redox potentials of the organic cofactor moiety between the enzymatic system and the model complexes has provided valuable insights into the role of the π–π stacking interaction in stabilization of the organic radical species [42,43].

4. Copper(II)–phenoxyl radical complexes (active form model)

Six types of Cu(II)–phenoxyl radical complexes have so far been reported as models of the active form of GAO (Table 3) [35,38,44–46]. Chemical or electro-

Table 3
Physicochemical properties of Cu(II)–phenoxyl radical complexes

Complex	λ_{max}/nm (ε/M^{-1} cm^{-1})	Raman band/ cm^{-1}	ESR	
			Cu complex	Phenoxyl radical
$[Cu^{II}(\mathbf{7}^{tBu2\bullet})(CH_3CN)]^{2+}$ [a]	410 (4000), 672 (1000)	1497	Silent	$g = 2.00$ for $\mathbf{7}^{tBu2\bullet}$ [b]
$[Cu^{II}(\mathbf{8}^{-\bullet})]^{+}$ [a]	398 (3900), 568 (2200), 646 (2200)	1495	Silent	– [c]
$[Cu^{II}(\mathbf{9}^{-\bullet})]^{+}$ [d]	– [e]	– [c]	Silent	$g = 2.0060$ for $\mathbf{9}^{-\bullet}$ [b]
$[Cu^{II}(\mathbf{10}^{\bullet})(NO_3^-)]^{+}$ [f]	415 (1790), 867 nm (550)	1512, 1589	Silent	$g = 2.0052$ for $\mathbf{10}^{\bullet}$ [b]
$[Cu^{II}(\mathbf{11}^{-})(\mathbf{12}^{\bullet})]^{+}$ [g]	419 (4400), 907 (1200), 1037 (1100)	– [c]	Silent	– [c]
$[Cu^{II}_2(\mathbf{13}^{-\bullet})_2]^{2+}$ [h]	404 (8000)	1451, 1579, 1594, 1606	Silent	– [c]
Active GAO	444 (5194), 800 (3211) [i]	1487, 1595, 1603 [i]	Silent [j]	$g = 2.005$ for $Tyr^{\bullet}$ [k,l]
Active GLO [i]	448 (5700), 851 (4300)	1486, 1590, 1604	Silent	$g = 2.0055$ for $Tyr^{\bullet}$ [k]

[a] Taken from Ref. [35].
[b] Phenoxyl radical of the Zn(II) complex.
[c] Not reported.
[d] Taken from Ref. [37,38].
[e] The anticipated phenoxyl radical absorption feature at ca. 400 nm is obscured by intense Schiff-base ligand absorption.
[f] Taken from Ref. [46].
[g] Taken from Ref. [44].
[h] Taken from Ref. [45].
[i] Taken from Ref. [19].
[j] Ref. [8].
[k] Oxidized form of apo-enzyme [Cu(II) free form].
[l] Taken from Ref. [10].

chemical one-electron oxidation of the corresponding Cu(II)–phenolate complexes has provided relatively stable Cu(II)–phenoxyl radical complexes. All the Cu(II)–phenoxyl radical complexes exhibit a characteristic absorption band around 400 nm, which appears in the somewhat lower wavelength region than that of the native enzymes (ca. 445 nm) [35,38,44–46]. One of the most characteristic features of the active form of GAO and GLO is an intense absorption band extending over the entire UV–vis–near IR spectral range [10]. This characteristic absorption band has been attributed mainly to a tyrosinate (Tyr^{-}495)–tyrosyl radical ($Tyr^{\bullet}$272) inter-ligand charge transfer transition [47]. However, such a characteristic absorption band has also been obtained in model complexes $[Cu^{II}(\mathbf{10}^{\bullet})(NO_3^-)]^+$ and $[Cu^{II}(\mathbf{11}^-)(\mathbf{12}^{\bullet})]^+$, which lack a second phenolate ligand in it (Fig. 5) [44,46]. On the other hand, the Cu(II) complexes containing additional phenolate group such as $[Cu^{II}(\mathbf{9}^{-\bullet})]^+$ and $[Cu_2^{II}(\mathbf{13}^{-\bullet})_2]^{2+}$ exhibited no such absorption band in the longer wavelength region [37,45].

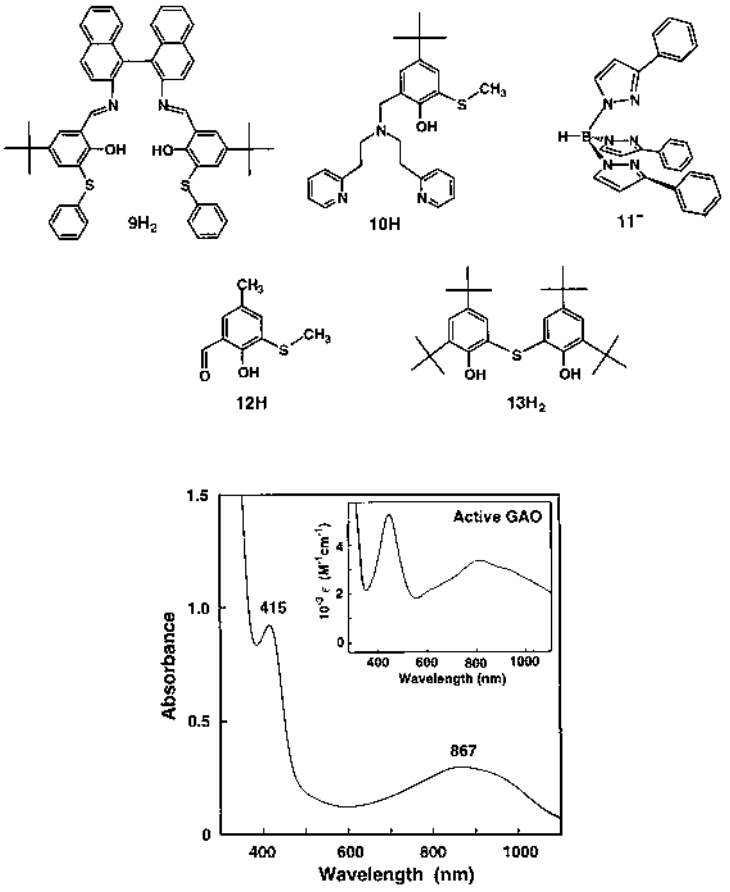

Fig. 5. UV-vis spectra of $[Cu^{II}(\mathbf{10}^{\bullet})(NO_3^-)]^+$ in CH_3CN [46]. Inset: UV-vis spectra of the active form of GAO [10].

These results suggest that the inter-ligand charge transfer is not the only process but π–π*, MLCT and/or LMCT transitions should also be taken into account [44]. On the basis of the spectroscopic and theoretical examinations on the metal-free phenoxyl radical species of the cofactor model compounds, we have attributed these broad absorption bands above 800 nm to the intramolecular charge transfer from the benzene ring to the methylthio groups in the phenoxyl radical species [28]. It is interesting to note that the position and strength of the broad absorption band in the visible to near IR region are significantly different in each Cu(II) complex, as shown in Table 3. The reason for such differences has yet to be clearly understood.

The Cu(II) complexes of phenoxyl radical species as well as the active form of GAO and GLO exhibit prominent peaks at around 1500 and 1600 cm^{-1} in the resonance Raman spectra [33,35]. These bands have been assigned to the modes ν_{7a} and ν_{8a} which predominantly include the C–O stretching and the C_{ortho}–C_{meta} stretching, respectively [33,35]. All the Cu(II) complexes of phenoxyl radical species are ESR silent, being consistent with magnetic coupling between the $S = 1/2$ Cu(II) ion and the $S = 1/2$ phenoxyl radical, although the type of coupling (antiferromagnetic or ferromagnetic) is unclear [35]. On the other hand, the Zn(II) complexes afford an isotropic ESR peak at $g = 2.0052$–2.0060, which are very close to those of the cofactor radicals (2.0055) in the enzyme active sites and also to that of the metal-free phenoxyl radicals of the model compounds (see, Table 2) [19,28]. Examination of the hfc values of the benzylic methylene protons of the phenoxyl radical species has indicated that the coordination geometry is not altered significantly upon one-electron oxidation of the phenolate to phenoxyl radical form in the Zn complex [36].

5. Alcohol-oxidation by phenoxyl radical complexes

$[Cu^{II}(\mathbf{9}^{-\bullet})]^{+}$ developed as a functional model of GAO has shown to catalyze oxidation of primary alcohols to the corresponding aldehydes [37,38]. Turnover numbers more than 10^3 has been achieved using O_2 as an electron acceptor [38]. A significantly distorted square planar coordination geometry with the N_2O_2 donor set was proposed to be essential for enhancing the substrate binding process and the alcohol-oxidation reaction [38]. Namely, the substrate binding leads to a five coordinate square pyramidal structure that is favorable to Cu(II) and the alcohol-oxidation leads to the Cu(I) complex with a four coordinate tetrahedral geometry, which is stabilized by the tetrahedrally distorted ligand environment [38]. A hydroperoxo–Cu(II) complex was proposed to be involved in the reaction of Cu(I)–phenol and dioxygen to generate Cu(II)–phenoxyl radical and H_2O_2 [38]. However, more comprehensive studies are required to know the mechanistic details of the alcohol-oxidation and the O_2-reduction processes.

$[Cu^{II}_2(\mathbf{13}^{-\bullet})_2]^{2+}$ can also oxidize alcohols catalytically under aerobic conditions [45]. In this reaction, only the phenoxyl radical sites in the dimer act as the oxidant but no redox reaction takes place at the Cu(II) site; thus, the two electrons from the alcohol substrate are accepted by two phenoxyl radical sites in the dimer. This

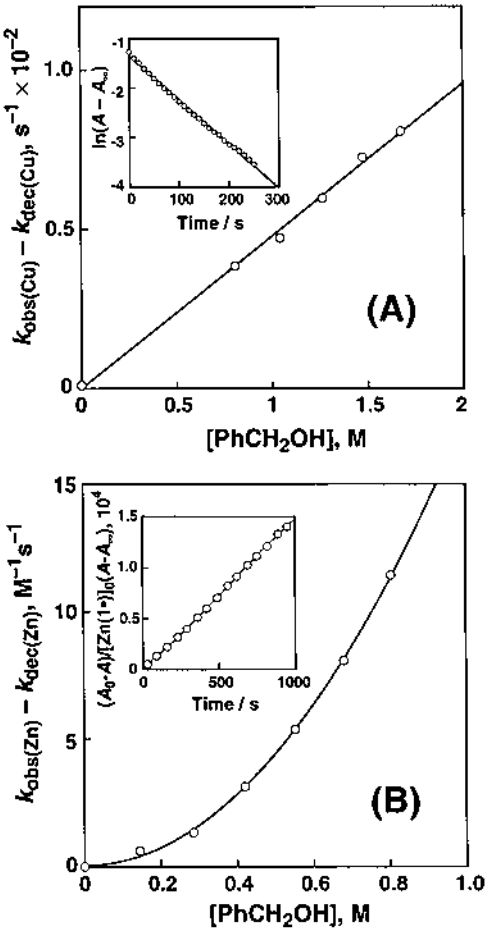

Fig. 6. (A) Plot of $(k_{obs(Cu)} - k_{dec(Cu)})$ vs. the benzyl alcohol concentration for the oxidation of benzyl alcohol by $[Cu^{II}(\mathbf{10^{\bullet}})(NO_3^-)]^+$ in CH_3CN at 25°C [46]. Inset: pseudo-first-order plot for the oxidation. (B) Plot of $(k_{obs(Zn)} - k_{dec(Zn)})$ vs. the benzyl alcohol concentration for the oxidation of benzyl alcohol by $[Zn^{II}(\mathbf{1^{\bullet}})(NO_3^-)]^+$ in CH_3CN at 25°C [46]. Inset: second-order plot for the oxidation. $k_{dec(Cu)}$ and $k_{dec(Zn)}$ are the rate constants of self-decomposition of the $[Cu^{II}(\mathbf{10^{\bullet}})(NO_3^-)]^+$ and $[Zn^{II}(\mathbf{10^{\bullet}})(NO_3^-)]^+$, respectively.

mechanism is quite different from that of the proposed enzymatic mechanism with respect to the redox behavior of Cu(II) [11–15].

We have recently succeeded in demonstrating the importance of the redox cycle of Cu(II) as well as that of phenoxyl radical site for the efficient two-electron oxidation of benzyl alcohol to benzaldehyde at a mononuclear Cu(II)–phenoxyl radical center in a model system [46]. Oxidation of benzyl alcohol by $[Cu^{II}(\mathbf{10^{\bullet}})(NO_3^-)]^+$ proceeded in CH_3CN at ambient temperature to yield benzaldehyde and $[Cu^{I}(\mathbf{10H})]^+$ quantitatively. The decay rate of $[Cu^{II}(\mathbf{10^{\bullet}})(NO_3^-)]^+$ monitored at 867 nm obeys *pseudo-first-order kinetics* and the plot of the

pseudo-first-order rate constant $k_{obs(Cu)}$ vs. the benzyl alcohol concentration gives a straight line as shown in Fig. 6(A). A large kinetic deuterium isotope effect ($k^{H}_{(Cu)}/k^{D}_{(Cu)} = 6.8$) was obtained when $PhCH_2OH$ was replaced by $PhCD_2OH$, indicating that the benzylic hydrogen atom abstraction is involved in the rate-determining step [46].

Oxidation of benzyl alcohol by $[Zn^{II}(\mathbf{10^{\bullet}})(NO_3^-)]^+$ yielded benzaldehyde as the oxidation by $[Cu^{II}(\mathbf{10^{\bullet}})(NO_3^-)]^+$. In contrast to the case of $[Cu^{II}(\mathbf{10^{\bullet}})(NO_3^-)]^+$, however, the decay rate of $[Zn^{II}(\mathbf{10^{\bullet}})(NO_3^-)]^+$ monitored at 887 nm due to the Zn(II) complex of the phenoxyl radical obeys *second-order kinetics*, and the second-order rate constant $k_{obs(Zn)}$ shows the *second-order dependence* on the alcohol concentration (Fig. 6(B)). Furthermore, the yield of benzaldehyde was nearly half of the yield of the copper case [46].

These results clearly show that the oxidation of benzyl alcohol by $[Cu^{II}(\mathbf{10^{\bullet}})(NO_3^-)]^+$ proceeds via the coordination of benzyl alcohol in the *monomeric form* by formally a $2e^-/2H^+$ mechanism to give benzaldehyde and $Cu^{I}(\mathbf{10H})$ quantitatively (Type I in Scheme 7) [46]. On the other hand, no redox reaction is expected at the Zn(II) site. In such a case, two electrons can only be accepted by phenoxyl radical sites in a *dimeric form* (Type II in Scheme 7) [46]. Thus, the reaction obeys second-order kinetics in the case of $[Zn^{II}(\mathbf{10^{\bullet}})(NO_3^-)]^+$. The latter mechanism of the zinc complex is very close to that of the Wieghardt's system mentioned above [45]. The enzymatic reaction has so far been considered to proceed via the Type I mechanism [11–15]. Thus, the different kinetic formulations between $[Cu^{II}(\mathbf{10^{\bullet}})(NO_3^-)]^+$ and $[Zn^{II}(\mathbf{10^{\bullet}})(NO_3^-)]^+$ clearly demonstrate the importance of the redox cycle between Cu(I) and Cu(II) as well as the interconversion

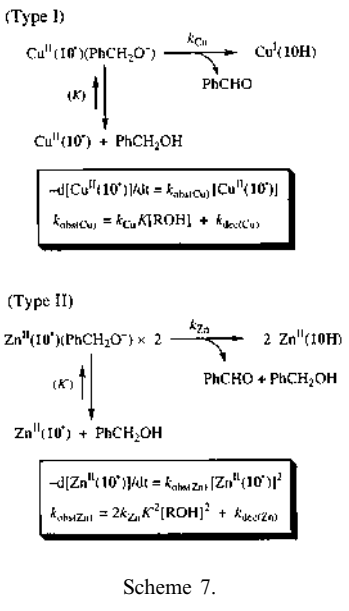

Scheme 7.

between the phenol and phenoxyl radical states for the efficient two-electron oxidation of alcohols at the *mononuclear copper site* of GAO which is fixed in the protein matrix.

6. Summary

In this mini review article, the recent model studies on the active sites of galactose oxidase (GAO) and glyoxal oxidase (GLO) have been summarized. Studies on the physicochemical properties of organic cofactor models in both the phenol (phenolate) and phenoxyl radical forms have indicated that the thioether group of the cofactor has the $2p\pi-3d\pi$ electron conjugative effect as well as the electron-donating nature, stabilizing the negative charge on the phenolate oxygen. The electron-sharing conjugative effect in the radical from has also been demonstrated by the ESR spectroscopy, electrochemical studies and the theoretical calculations.

A series of Cu(II) complexes of phenolates and phenoxyl radicals of the cofactor models have also been developed to uncover the important role of the metal ion center both on the spectroscopic features and on the redox functions of GAO and GLO. It has been demonstrated that the copper ion acts not only as the one-electron redox center but also as a catalytic center to enhance the reactivity of the phenoxyl radical species for the alcohol oxidation. The $\pi-\pi$ stacking interaction between Trp 290 and Tyr 272 in the enzyme active site has also been suggested to play important role for the enzymatic reactions [6,7], which has yet to be fully understood in the model systems.

References

[1] J. Stubbe, W.A. van der Donk, Chem. Rev. 98 (1998) 705.
[2] J. Stubbe, P. Riggs-Gelasco, Trends in Biochemical Science 23 (1998) 438.
[3] J.Z. Pedersen, A. Finazzi-Agrò, FEBS Lett. 325 (1993) 53.
[4] G. Avigad, D. Amaral, C. Asensio, B.L. Horecker, J. Biol. Chem. 237 (1962) 2736.
[5] D.J. Kosman, in: R. Lontie (Ed.), Copper Proteins and Copper Enzymes, vol. 2, CRC Press, Boca Raton, FL, 1985, pp. 1–26.
[6] N. Ito, S.E.V. Phillips, C. Stevens, Z.B. Ogel, M.J. McPherson, J.N. Keen, K.D.S. Yadav, P.F. Knowles, Nature 350 (1991) 87.
[7] N. Ito, S.E.V. Phillips, K.D.S. Yadav, P.F. Knowles, J. Mol. Biol. 238 (1994) 794.
[8] M.M. Whittaker, J.W. Whittaker, J. Biol. Chem. 263 (1988) 6074.
[9] M.M. Whittaker, V.L. DeVito, S.A. Asher, J.W. Whittaker, J. Biol. Chem. 264 (1989) 7104.
[10] M.M. Whittaker, J.W. Whittaker, J. Biol. Chem. 265 (1990) 9610.
[11] M.M. Whittaker, J.W. Whittaker, Biophys. J. 64 (1993) 762.
[12] M.M. Whittaker, D.P. Ballou, J.W. Whittaker, Biochemistry 37 (1998) 8426.
[13] B.P. Branchaud, M.P. Montague-Smith, D.J. Kosman, F.R. McLaren, J. Am. Chem. Soc. 115 (1993) 798.
[14] R.M. Wachter, B.P. Branchaud, Biochemistry 35 (1996) 14425.
[15] R.M. Wachter, M.P. Montague-Smith, B.P. Branchaud, J. Am. Chem. Soc. 119 (1997) 7743.
[16] K. Clark, J.E. Penner-Hahn, M.M. Whittaker, J.W. Whittaker, J. Am. Chem. Soc. 112 (1990) 6433.
[17] K. Clark, J.E. Penner-Hahn, M.M. Whittaker, J.W. Whittaker, Biochemistry 33 (1994) 12553.
[18] P.J. Kersten, Proc. Natl. Acad. Sci. USA 87 (1990) 2936.

[19] M.M. Whittaker, P.J. Kersten, N. Nakamura, J. Sanders-Loehr, E.S. Schweizer, J.W. Whittaker, J. Biol. Chem. 271 (1996) 681.
[20] P. Bork, R.F. Doolittle, J. Mol. Biol. 236 (1994) 1277.
[21] A. Harriman, J. Phys. Chem. 91 (1987) 6102.
[22] A. Boussac, A.L. Eteinne, Biochim. Biophys. Acta 766 (1984) 576.
[23] W. Tagaki, in: S. Oae (Ed.), Organic Chemistry of Sulfur, Plenum Press, New York, 1977, pp. 231–302.
[24] G.T. Babcock, M.K. El-Deeb, P.O. Sandusky, M.M. Whittaker, J.W. Whittaker, J. Am. Chem. Soc. 114 (1992) 3727.
[25] G.J. Gerfen, B.F. Bellew, R.G. Griffin, D.J. Singel, C.A. Ekbergand, J.W. Whittaker, J. Phys. Chem. 100 (1996) 16739.
[26] M.M. Whittaker, Y.-Y. Chuang, J.W. Whittaker, J. Am. Chem. Soc. 115 (1993) 10029.
[27] S. Itoh, K. Hirano, A. Furuta, M. Komatsu, Y. Ohshiro, A. Ishida, S. Takamuku, T. Kohzuma, N. Nakamura, S. Suzuki, Chem. Lett. (1993) 2099.
[28] S. Itoh, S. Takayama, R. Arakawa, A. Furuta, M. Komatsu, A. Ishida, S. Takamuku, S. Fukuzumi, Inorg. Chem. 36 (1997) 1407.
[29] S. Oae, M. Yoshihara, W. Tagaki, Bull. Chem. Soc. Jpn. 40 (1967) 951.
[30] G.N.R. Tripathi, R.H. Schuler, J. Phys. Chem. 92 (1988) 5129.
[31] In this article, we have mainly focused on the copper complexes containing a methylthio substituted phenol group as the active site model for GOase. Thus, the majority of the papers that deal with the copper complexes containing other phenol derivatives are not included here without some exceptions.
[32] M.M. Whittaker, W.R. Duncan, J.W. Whittaker, Inorg. Chem. 35 (1996) 382.
[33] R. Schnepf, A. Sokolowski, J. Müller, V. Bachler, K. Wieghardt, P. Hildebrandt, J. Am. Chem. Soc. 120 (1998) 2352 and Refs. cited therein.
[34] J.A. Halfen, V.G. Young Jr., W.B. Tolman, Angew. Chem. Int. Ed. Engl. 35 (1996) 1687.
[35] J.A. Halfen, B.A. Jazdzewski, S. Mahapatra, L.M. Berreau, E.C. Wilkinson, L. Que Jr., W.B. Tolman, J. Am. Chem. Soc. 119 (1997) 8217.
[36] A. Sokolowski, J. Müller, T. Weyhermüller, R. Schnepf, P. Hildebrandt, K. Hidenbrand, E. Bothe, K. Wieghardt, J. Am. Chem. Soc. 119 (1997) 8889.
[37] Y. Wang, T.D.P. Stack, J. Am. Chem. Soc. 118 (1996) 13097.
[38] Y. Wang, J.L. DuBois, B. Hedman, K.O. Hodgson, T.D.P. Stack, Science 279 (1998) 537.
[39] N. Kitajima, K. Whang, Y. Moro-oka, A. Uchida, Y. Sasada, J. Chem. Soc. Chem. Commun. (1986) 1504.
[40] H. Adams, N.A. Bailey, I.K. Campbell, D.E. Fenton, Q.-Y. He, J. Chem. Soc. Dalton Trans. (1996) 2233.
[41] M. Vaidyanathan, R. Viswanathan, M. Palaniandavar, T. Balasubramanian, T.P. Muthiah, Inorg. Chem. 37 (1998) 6418.
[42] M. Ruf, C.G. Pierpont, Angew. Chem. Int. Ed. Engl 37 (1998) 1736.
[43] M.A. Halcrow, E.J.L. McInnes, F.E. Mabbs, I.J. Scowen, M. McPaetlin, H.R. Powell, J.E. Davis, J. Chem. Soc. Dalton Trans. (1997) 4025.
[44] M.A. Halcrow, L.M.L. Chia, X. Liu, E.J.L. McInnes, L.J. Yellowlees, F.E. Mabbs, J.E. Davies, Chem. Commun. (1998) 2465.
[45] P. Chaudhuri, M. Hess, U. Florke, K. Wieghardt, Angew. Chem. Int. Ed. Engl. 37 (1998) 2217.
[46] S. Itoh, M. Taki, S. Takayama, S. Nagatomo, T. Kitagawa, N. Sakurada, R. Arakawa, S. Fukuzumi, Angew Chem. 111 (1999) 2944; Angew Chem. Int. Ed. Engl. 38 (1999) 2774.
[47] M.L. McGlashen, D.D. Eads, T.G. Spiro, J.W. Whittaker, J. Phys. Chem. 99 (1995) 4918.